



# Multi-scale morphodynamics of an estuarine beach adjacent to a flood-tide delta: Assessing decadal scale erosion

Daniel L. Harris<sup>a,b,\*</sup>, Ana Vila-Concejo<sup>c</sup>, Timothy Austin<sup>d</sup>, Javier Benavente<sup>e</sup>

<sup>a</sup> School of Earth and Environmental Sciences, The University of Queensland, Brisbane, Queensland, 4072, Australia

<sup>b</sup> Remote Sensing Research Centre, The University of Queensland, Brisbane, Queensland, 4072, Australia

<sup>c</sup> Geocoastal Research Group, School of Geosciences, University of Sydney, NSW, 2006, Australia

<sup>d</sup> Coastal and Regional Oceanography Lab, School of Mathematics and Statistics, University of New South Wales (UNSW), Sydney, NSW, 2052, Australia

<sup>e</sup> Department of Earth Sciences, Faculty of Marine and Environmental Sciences, University of Cádiz, 11510, Puerto Real, Cadiz, Spain

## ABSTRACT

Estuarine beaches are ubiquitous, yet understudied, coastal systems. The mixed hydrodynamic processes – such as combined tidal and wave forcing – and the influence of adjacent sedimentary features – such as flood-tide deltas (FTDs) – leads to complex morphodynamic processes. As such, the dynamics and evolution of these important coastal systems are poorly understood. This study synthesises a set of analyses conducted on an estuarine beach, in southeast Australia, over multiple temporal scales. Nearshore waves and currents were measured and used to determine the processes driving seasonal to yearly beach change between 2007 and 2010. These results were compared to decadal scale beach change determined from aerial photos between 1963 and 2006. We found the westward transport of sediment towards the inner estuary was the dominant nearshore process leading to erosion in the eastern regions of the beach (near the estuary entrance) and accretion in the west over yearly time scales. Cross-shore sediment transport occurred during winter storm swell conditions leading to erosion in more exposed sites and some limited accretion in sheltered zones, most likely due to sediment input from the flood-tide delta. However, severe storm swell events that propagated into the estuary led to a loss of sediment and erosion across the entire beach which was not recovered during the study period. It is likely that the erosion processes observed in the short- to medium-term (days to years) analyses are the conditions that led to the long-term shoreline retreat observed in the aerial photograph record. The long-term shoreline retreat since 1963 is likely a result of a negative sediment balance due to movement of the FTD and a lack of sediment input in the eastern regions of Shoal Bay. Shoreline retreat will likely continue unless increased sediment input occurs from marine sources or shoreline interventions are maintained.

## 1. Introduction

Estuarine beaches are ubiquitous coastal features. Their combined length far exceeds that of oceanic (open coast) shorelines, yet there are relatively few morphodynamic studies on estuarine beaches, or low-energy beaches in general, when compared to wave-dominated open coast environments (Travers, 2007; Vila-Concejo et al., 2019, 2010). Estuarine beaches are a sub-class of beaches classified as low-energy (e.g. Jackson et al., 2002) or reflective (e.g. Short, 2006). Studies that have specifically focused on low-energy estuarine beaches show that they are hydrodynamically complex when compared to beaches on wave-dominated open coasts (Nordstrom et al., 2003). Most of the processes that drive open coast beach change under normal conditions (such as rip currents and surf zones) are absent. Instead mechanisms that are usually secondary in the surf zone (such as tidal currents) become important drivers in beach change and long-term evolution (Jackson et al., 2002). This is due, in part, to the typical geographical settings of estuarine beaches; in fetch-limited, swell attenuated and/or tidal

dominated environments (Jackson et al., 2002).

A number of studies have attempted to link local hydrodynamics to estuarine beach morphology conceptually – in a similar way to the Wright and Short (1984) beach model for wave dominated environments – with limited success (e.g. Hegge et al., 1996; Makaske and Augustinus, 1998; Sanderson et al., 2000; Travers, 2007). Models that solely focus on the beach geomorphology have been produced that, for example, define low-energy beaches by profile shape (Hegge et al., 1996). However, deciphering links between beach type and nearshore dynamics remains elusive (Bernabeu et al., 2012). The difficulty in linking near-modal hydrodynamic conditions to beach morphology in low-energy environments is often due to the occurrence of relict morphologies, such as storm erosion scarps and beach cusps (Costas et al., 2005; Jackson et al., 2002). As a result the morphology of the beach does not entirely reflect the day-to-day hydrodynamic conditions making it difficult to construct morphodynamic links between hydrodynamics and morphology (Hegge et al., 1996).

The sediment dynamics of low-energy environments can also be

\* Corresponding author. School of Earth and Environmental Sciences, The University of Queensland, Brisbane, Queensland, 4072, Australia.

E-mail address: [daniel.harris@uq.edu.au](mailto:daniel.harris@uq.edu.au) (D.L. Harris).

<https://doi.org/10.1016/j.ecss.2020.106759>

Received 21 March 2019; Received in revised form 2 April 2020; Accepted 7 April 2020

Available online 29 April 2020

0272-7714/© 2020 Elsevier Ltd. All rights reserved.

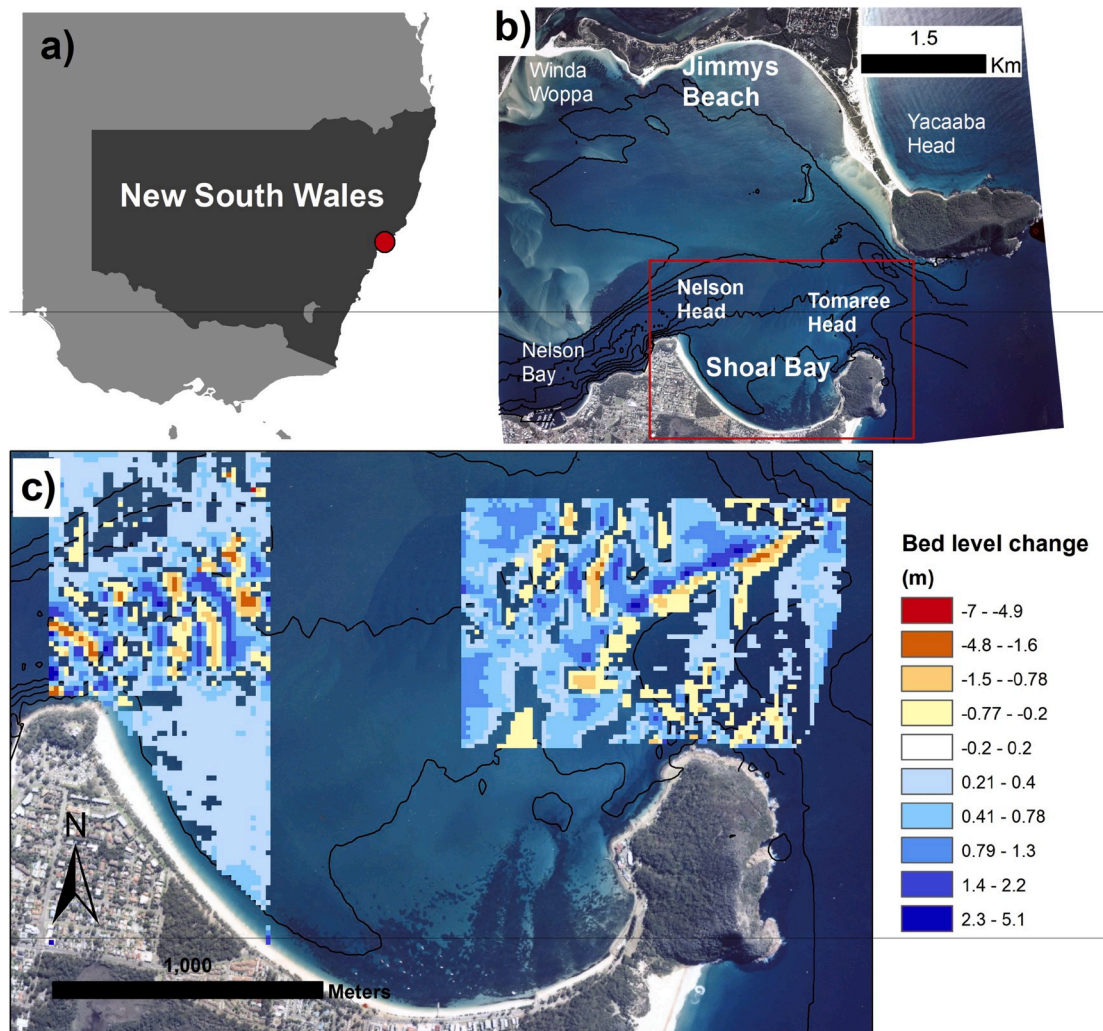


**Fig. 1.** (a) Location of Port Stephens, NSW, Australia, shown as the red dot; (b) aerial photo of the lower estuarine environment (April 2006) showing the main morphological features. Contours of 5 m intervals are also shown as black lines; (c) study site of Shoal Bay is located on the southern shoreline, with results from vertical seabed change calculations between the 2007 and 2010 bathymetric surveys. Sediment erosion observed between the two surveys is shown in Table 2. (For interpretation of the references to colour in this figure legend, the reader is referred to the Web version of this article.)

more complex due to the geographical location of such systems (Jackson et al., 2002). Low-energy beaches are often associated with, or found within, larger coastal systems such as estuaries, lagoons and in lee of islands, reefs or other barriers (Jackson et al., 2002). Substantial dissipation of swell wave energy usually occurs in such settings prior to reaching low-energy shorelines. Local wind driven wave heights are also relatively small because fetch distance is limited by the extent and orientation of surrounding coastal formations, such as reefs, or the estuary/bay itself. As a result, their morphodynamics are connected to the evolution of the geological setting, such as behind coral or rocky reefs, and adjacent sediment morphologies such as flood-tide deltas (FTDs) (Roy, 1984, 2001; Vila-Concejo et al., 2011b). On short-term time scales, the links between low-energy beach dynamics adjacent coral reefs and ebb-tide deltas are well studied (e.g. Backstrom et al., 2008; Brander et al., 2004; Kench and Brander, 2006; Kench and McLean, 2004; Tātui et al., 2014; Webb, 2006a, b; Winter et al., 2017). However, few studies have focused on the interactions between estuarine beaches and FTDs on yearly to decadal time scales (e.g. Austin et al., 2018), with most of our understanding based on centennial to millennial scales (Cowell et al., 1995; Karunaratna et al., 2008; Roy et al., 1980). This is crucial since marine sediment input to estuarine beaches is dependent on sediment exchange with FTDs on many wave dominated coasts (Cowell et al., 1995).

FTDs are sediment deposits formed on the landward side of tidal inlets and wave-dominated estuaries by the incoming flood tide currents and ocean waves (Hayes, 1975, 1980). FTDs are ubiquitous features on wave-dominated micro-tidal settings with long-term stable sea levels, minimal fluvial processes, and where the geological setting allows for deep embayments and a high accommodation space (Perillo and Piccolo, 2011; Roy et al., 1980). Yet, their morphodynamics are rarely investigated when compared to ebb-tide deltas (Austin et al., 2018). They are considered sediment “sinks” that will collect marine sediment until the accommodation space of the estuary, or the marine sediment source, is depleted (Dalrymple et al., 1992; Roy et al., 1980). Hayes (1975, 1980) and Boothroyd (1985) investigated the dynamics of FTDs and found that the shallower regions of FTDs are flood dominated and deeper channels are ebb dominated. The shallow and channel regions of the FTDs are further differentiated by Hayes (1980) into flood ramps which terminate at shoals or ebb shields. Regions that surround the flood-ramps are ebb-dominated with sediment transport and current flow mostly towards the estuarine entrance. Roy et al. (1980) and Roy et al. (2001) examined the millennial evolution of estuaries and FTDs on the south-east Australian coast and found that, in this setting, FTDs migrate away from the estuarine entrance due to wave and tide processes. This finding was supported by recent research by Austin et al. (2018). Over Holocene time scales FTD migration is offset by sediment input from the marine

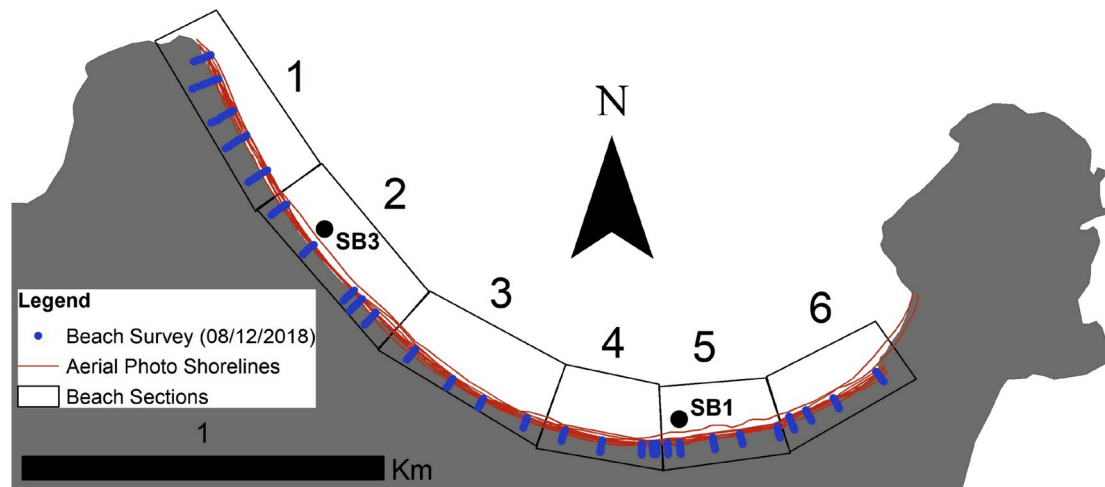


**Fig. 2.** Beach sections used in assessing shoreline change for both aerial photographs and beach surveys and hydrodynamic deployment locations. Locations of beach profile surveys are shown as blue dots and the shorelines derived from the aerial photos are also shown in red. (For interpretation of the references to colour in this figure legend, the reader is referred to the Web version of this article.)

environment leading to FTDs acting as net sediment sinks (Roy et al., 1980). In instances where sediment input is reduced FTDs either migrate upstream with erosion on the seaward face or lead to retreat of adjacent shorelines (Roy et al., 1980). Conceptual models for redistribution of sediment in FTDs, where they exist, vary between estuaries, with potential impacts on adjacent estuarine beaches further complicated by varying degrees of beach-FTD connectivity (e.g. Austin et al., 2018). For example, sediment exchange can occur easily when the FTD (or other tidal shoals) abut beaches; on the other hand, where a deep channel abuts the beach, the sediment eroded during high-energy conditions may be lost to the beach system (Vila-Concejo et al., 2019). Therefore, little is known of the links between processes that act on shorter time scales in estuaries – such as seasonal or decadal wave climate change or shoreline retreat – to the changes in broader estuary and FTD morphology (Karunaratna et al., 2008). This obscures development of a single description of FTD and beach morphodynamics.

This study collates a suite of data sets from field campaigns between 2007 and 2010 and aerial images from 1963 to 2006 at Port Stephens, New South Wales, Australia. It examines the evolution of an estuarine beach on a wave-dominated coast bounded by two headlands and flanked by a well-developed FTD in SE Australia. A multi-scale (days to decadal) approach is taken to assess the local and regional processes that affect shoreline evolution. Considering the prominence of low-energy estuarine beaches flanked by FTDs in or near capital cities (e.g. Sydney, San Francisco, and many more), our study is directed towards a significant knowledge gap for estuarine beaches located on wave dominated coasts globally. The aims for the study are: a) to investigate the likely conditions that lead to erosion or accretion of an estuarine beach, adjacent to a well-developed flood-tide delta, over multiple temporal scales; and, b) to provide a broader understanding of estuarine beach morphodynamics on wave-dominated coasts.

## 2. Study site

Port Stephens estuary is a ria-like drowned river valley located approximately 230 km north of Sydney, New South Wales, Australia (Fig. 1). It is a tide dominated estuary on a high-energy coast, with a well-developed FTD typical of a high-energy environment (Vila-Concejo et al., 2007). Most of the shoreline within Port Stephens falls within the low-energy classification of Jackson et al. (2002). Process-based assessments (Austin et al., 2018; Austin et al., 2009; DPWS, 1999; Vila-Concejo et al., 2011b, 2010; 2009) and studies on historic evolution (DPWS, 2000; PWD, 1985, 1987; Thom et al., 1992; Vila-Concejo et al.,

2011b, 2010; 2007) have shown substantial FTD and shoreline change over seasonal to yearly periods.

The wave regime for the open coast in this region is classified as moderate with mean offshore significant wave heights ( $H_{so}$ ) of 1.5 m and an associated period ( $T_{so}$ ) of 8 s (Short and Trenaman, 1992). Storm conditions mostly occur during the winter from the E-SE (Short and Trenaman, 1992).

The long-term evolution of the outer zone of Port Stephens shows that some regions have accumulated marine sediment or migrated (Fig. 1): (a) Winda Woppa spit (Vila-Concejo et al., 2011b); and (b) Yacaaba sandwave (Vila-Concejo et al., 2007, 2009). Conversely, the Port Stephens shorelines eroded over the past 50 years which has triggered numerous shoreline intervention strategies (DPWS, 1999, 2000; PWD, 1979, 1985; 1987; Vila-Concejo et al., 2007).

The conceptual model for the Port Stephens FTD, developed by Austin et al. (2018), shows that the shallow regions of the FTD are dominated by flooding currents and the deeper channels by ebb currents, in support of the concepts outlined by Hayes (1980). Austin et al. (2018) further showed that the progressive westward migration of the FTD and erosion of the flood-ramp most likely results in a net sediment loss to the beaches. These results were derived from a combination of tidal current measurements in the estuary and repeat bathymetric surveys across important features in the flood-tide delta.

Shoal Bay is the most easterly and energetic beach on the southern shoreline of Port Stephens (Fig. 1c). It is a 2.5 km long embayed low-energy estuarine beach most exposed to ocean swell at its western end (Short, 2007). The higher energy wave conditions at the western end of the beach is reflected in the beach geomorphology. Pronounced beach cusps occur in this region whose spacing and size are best described by the wave process models of beach cusp formation (Benavente et al., 2011). Several engineering interventions were conducted between 1986 and 2000 to address erosion issues, including the placement of approximately 83,000 m<sup>3</sup> of sand. Some shoreline control interventions occurred prior to 1986, however documentation of these projects is scarce. Since 2000 emergency nourishments have occurred regularly, involving the removal of sediment from the western end of the beach and the placement on the eastern end as well as nourishment from external sources. Details of the exact volume of sediment used and timing of beach nourishment in Shoal Bay is unknown, however, it is likely that trends in shoreline change during our study period (1963–2010) have been influenced by shoreline protection interventions and beach nourishment.



### 3. Methods

The morphodynamics of Shoal Bay were assessed over three temporal scales. The methods and results below are therefore partitioned into the three scales of: short-term (seconds to days), medium-term (days to years), and long-term (years to decades).

#### 3.1. Hydrodynamic surveys

Two intensive field campaigns in winter (22nd–24th July) and summer (13–14th and 16–17th December) were undertaken in 2008. These included measurement of nearshore hydrodynamics using current meters (Acoustic Doppler Velocimeters, ADVs) and pressure transducers (PTs). There were two deployment locations in the nearshore zone in the east (SB1) and west (SB3) of the Shoal Bay embayment (Fig. 2). The current meter at a location between the east and west deployments (SB2) failed in the summer field campaign and was thus not included in the subsequent analysis. The PTs were measuring continuously at 10 Hz and were kept within 1 m of the water surface throughout the tidal cycle to remove the influence of pressure attenuation with depth. Waves from the PTs were calculated according to the methods outlined in detail in Harris et al. (2018). The ADVs were deployed so they were sampling at less than 20 cm from the sea floor and they were oriented with one axis perpendicular to the incoming waves. Measurements were taken every half hour for 15 min at 5 Hz.

##### 3.1.1. Sediment entrainment

Sediment entrainment was calculated using the method of Vila-Concejo et al. (2010). The orientation of the current meters allowed us to assume that the oscillatory measurements that were taken in the cross-shore direction corresponded to the near-bed wave orbital velocities that cause sediment entrainment. The directly measured peak near bed orbital velocity ( $U_w$ ) ( $\text{ms}^{-1}$ ) and its associated frequency ( $F$ ) ( $\text{Hz}$ ) were used to determine the peak orbital excursion ( $A$ ) ( $\text{ms}^{-1}$ , Eq. (1)), relative roughness ( $r$ , Eq. (2)) and wave friction factor ( $f_w$ , Eq. (3)):

$$A = U_w F / 2\pi \quad \text{Eq. 1}$$

$$r = A / k_s \quad \text{Eq. 2}$$

$$f_w = 0.237 r^{-0.52} \quad \text{Eq. 3}$$

where,  $k_s$  is Nikuradse roughness length ( $2.5 \times D_{50}$ ) for the flat marine sands (Soulsby, 1997) and  $D_{50}$  is the mean grain size in metres ( $D_{50} = 406 \mu\text{m}$  at SB1,  $D_{50} = 412 \mu\text{m}$  at SB3).

Critical shear stress ( $\tau_{cr}$ , Eq. (6)) and critical velocity amplitude ( $U_{cr}$ ) ( $\text{ms}^{-1}$ , Eq. (7)) were then determined based on Soulsby (1997) using Equations (4)–(7):

$$D^* = D_{50} \left[ \frac{g(s-1)}{(\nu^2)^{\frac{1}{3}}} \right] \quad \text{Eq. 4}$$

$$\theta_{cr} = [0.30 / 1 + 1.2D^*] + 0.055[1 - \exp(-0.02D^*)] \quad \text{Eq. 5}$$

$$\tau_{cr} = \theta_{cr} g (\rho - \rho_s) D_{50} \quad \text{Eq. 6}$$

$$U_{cr} = \sqrt{2\tau_{cr} / \rho f_w} \quad \text{Eq. 7}$$

where  $\rho$  is water density ( $1027 \text{ kg/m}^3$ ),  $\rho_s$  is the sediment density ( $2650 \text{ kg/m}^3$ ),  $s$  is ratio of sediment to water density ( $\rho_s/\rho$ ),  $g$  is the gravitational acceleration ( $9.8 \text{ ms}^{-2}$ ) and  $\nu$  is the kinematic viscosity of water ( $1.1 \times 10^{-6} \text{ m}^2\text{s}^{-1}$ ).

Currents exceeding the critical velocity amplitude were deemed capable of entraining sediment. The percentage of entrainment ( $E$ ) was computed using Eq. (8) and represents how often the surveyed nearshore currents have the capability to entrain sediment from the bed.

$$E = (C_f / C) \times 100 \quad \text{Eq. 8}$$

where,  $C_f$  is the duration for which the sampled nearshore currents were above  $U_{cr}$ ; and  $C$  is the total duration of the deployment.

##### 3.1.2. Residuals: current and percentage of entrainment

Residual current velocities were averaged over the 15 min runs to determine the dominant direction of the longshore current velocity. Direction of alongshore net residual flow was determined by modifying the Black et al. (1989) residual distance formula ( $R_f$ , Eq. (9))

$$R_f = (d_w \times v_w) - (d_e \times v_e) \quad \text{Eq. 9}$$

where,  $d_w$  and  $d_e$  are the duration of currents in the west and east directions respectively and  $v_w$  and  $v_e$  the longshore velocity towards the west and east.  $R_f$  is the residual distance of current flow over the deployment period.

A similar approach was taken in determining the direction of current flow producing the most entrainment.  $E_f$  was derived by using the nearshore current residuals towards the east and the west for each 15 min recording and their associated values of  $E$  where

$$E_f = (d_w \times E_w) - (d_e \times E_e) \quad \text{Eq. 10}$$

$E_w$  corresponds to the average values of  $E$  associated with westward residual currents and  $E_e$  with eastwards.

#### 3.2. Topographic and bathymetric surveys

##### 3.2.1. Beach surveys

Beach surveys were conducted periodically using a Trimble R8 RTK-GNSS (Real Time Kinematic Global Navigation Satellite System) from May 2008 to January 2010. A total of 23 profiles were taken approximately every 100–200 m along the entire beach. Each beach survey started from the same location which was the top of the foredune scarp or berm. We used linear volumes to determine beach change since this was the most accurate method of comparing change at the different sites although some data is lost for sediment transported below 0 m. Linear volumes ( $\text{m}^3/\text{m}$ ) were computed from the toe of the fore-dune to the 0 m Australian Height Datum (AHD) line, where AHD is approximately equal to Mean Sea Level (MSL). The cross-sectional area of the beach profile above the 0 AHD line was used to calculate linear volume. 0 AHD was used as a baseline since it is comparable across profiles and it was crossed by all beach profiles. The area above AHD was calculated using the trapezoidal numerical integration functions in MATLAB®. Six sections were defined along the beach to analyse volumetric changes (Fig. 2). Linear volumes averaged for each section and total volumes were calculated by multiplying the average linear volume with the alongshore length of the section. Volume change for each section ( $Vi(t)$ ) was then normalised between 0 and 1 based on the maximum and minimum volumes for each section (Eq. (11)).

$$Vi(t) = (Vi(t) - \min(Vi)) / (\max(Vi) - \min(Vi)) \quad \text{Eq. 11}$$

This allowed for easier and direct comparison of shoreline change between each section by removing the influence of the different relative volumes and trends within time series data sets. Additional alongshore beach profiles in areas with rhythmic topography were taken in conjunction with the 23 cross-shore profiles in order to develop a three dimensional representation of Shoal Bay. A DEM of Shoal Bay from the 2010 survey, detailing the three dimensional rhythmic features of the beach, was construct in Esri ArcGIS® ArcMap™ 10.6.1.

##### 3.2.2. Bathymetric surveys

Two bathymetric surveys were conducted 28 months apart in October 2007 and in February 2010. Methods and results from bathymetric surveys most relevant for Shoal Bay are outlined here, however, for full details see Austin et al. (2018). The survey in 2007 was

conducted by the New South Wales Office of Environment and Heritage (OEH) and utilised a single beam 200 kHz echo sounder in conjunction with a differential GPS (DGPS) and heave compensator. Measurements were taken continuously outputting every 20 m. Results from this survey were tidally corrected to the tide gauge situated at Tomaree Head (Fig. 1b). The 2010 survey was conducted using a single beam 200 kHz Cee HydroSystems™ Ceestar echo sounder with spatial coordinates supplied by a RTK-GNSS negating the need for tidal compensation. The Ceestar echo sounder was logging continuously at 6 Hz which were then averaged to 1 Hz during post processing. The 2010 survey followed the survey lines of the 2007 survey to minimise inaccuracies in the subsequent transformation to a  $16 \times 16$  m bathymetric grid. Austin et al. (2018) found that the maximum vertical accuracy of these surveys was about 0.15–0.2 m.

Two FTD morphological features were selected for bathymetric analysis. These are the ebb channel immediately off the western end of Shoal Bay and the ebb shoal located near Tomaree Head (Fig. 1). Vertical sea bed change assessments were conducted between the 2007 and 2010 bathymetric surveys. Volume changes that resulted from a vertical change of less than 0.2 m were removed and an average bed elevation change (m) was calculated by dividing the net volume change ( $\text{m}^3$ ) by the total area ( $\text{m}^2$ ). This method ignores small changes in vertical sea bed change and the bias this introduces, such as overlooking sea bed deflation, should be considered when interpreting the results. Annual rates of change ( $\text{myr}^{-1}$ ) were then calculated by dividing the average bed elevation change with the period between the two surveys. As the bathymetric surveys only provide two time points the volume change of the FTD provides a snapshot during the survey period but long-term trends are not decipherable. The results are presented here to offer a possible interpretation of sediment movements in the Port Stephens estuary and how this may affect Shoal Bay. Future research could monitor bathymetric change of the FTD and beaches over a longer time series which would more accurately detail the sediment dynamics between the FTD and adjacent beaches.

### 3.3. Aerial image and offshore wave analysis

Aerial photographs of Shoal Bay covered the period between 1963 and 2006; photos from 1963, 1977, 1986, 1991, 1994, 1996, 1999, 2001 and 2006 were used for this study. The waterline, or instantaneous shoreline, was used to determine shoreline position in each photograph. The photographs were all of similar resolution and the potential error introduced by the spring tidal range is approximately  $\pm 7$  m. Analysis of shoreline change along the entire beach was conducted using the Digital Shoreline Analysis System (DSAS) (Thieler et al., 2009) and 50 equidistant transects. Shoreline displacement results were then averaged for each beach section and for the entire beach (Fig. 2).

Offshore wave data from May 2008 to March 2010 was obtained from OEH through the Manly Hydraulics Laboratory (MHL) for the Crowdy Head wave rider buoy, 115 km north of the study site. These data included significant wave height and wave period. Long term storm records were obtained from the Sydney wave rider buoy which was used instead of the Crowdy Head buoy since it recorded wave direction and has a longer temporal record. Data from the Sydney buoy included date of the storm (defined as conditions where  $H_{s0} > 3$  m), hourly storm wave power ( $\text{J ms}^{-1}$ ), and the duration of the storm (h). These data were then converted into total wave power for each storm by multiplying hourly storm wave power by the duration of the storm in hours. The threshold of  $H_{s0} > 3$  m is used to define storms events in many previous studies on the Southeast coast of Australia (e.g. Harley et al., 2010; Lord and Kulmar, 2001; Shand et al., 2010) and has been shown to substantially change sedimentary formations on the northern shoreline of Port Stephens previously (Vila-Concejo et al., 2010)

**Table 1**

Average significant wave height and period ( $H_s$  and  $T$  respectively), sediment entrainment ( $E_f$ ) and residual current factor ( $R_f$ ) for each station during each fieldwork campaign. Positive values in the  $R_f$  and  $E_f$  results indicate a westward trending residual and negative eastwards.

Field Campaign	Station	Wave		Residuals	
		$H_s$ (m)	$T$ (sec)	$R_f$	$E_f$
Summer	East (SB1)	0.16	8.62	1.13	-0.57
	West (SB3)	0.36	8.26	2.23	2.78
Winter	East (SB1)	0.31	11.07	-0.09	0.29
	West (SB3)	0.56	9.98	2.17	1.42

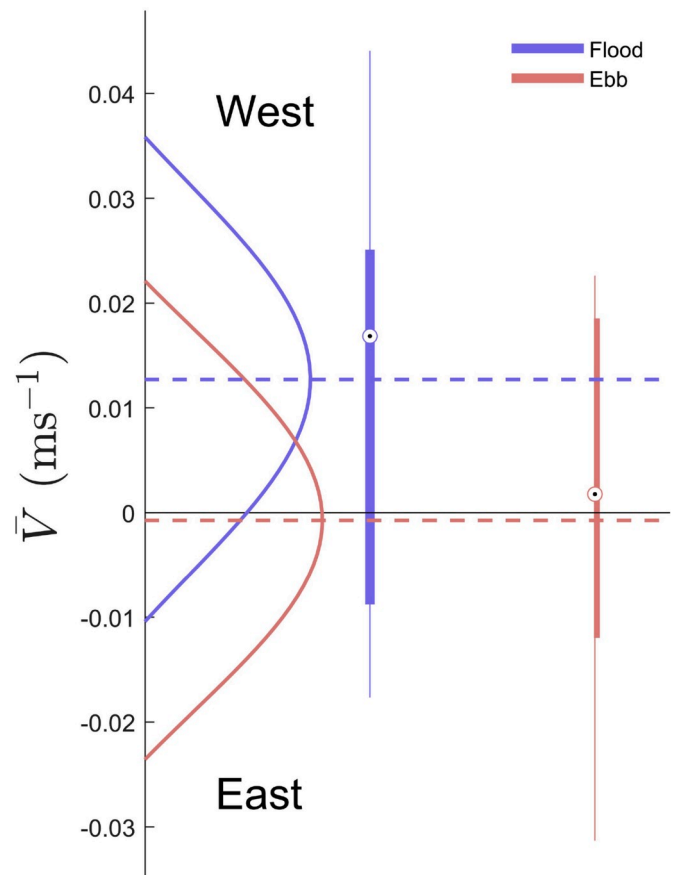


**Fig. 3.** Box and whisker plots with corresponding probability density functions as solid lines showing the average hourly current velocities ( $\bar{V}$ ) across summer and winter from both deployment locations and during flood and ebb tidal flows. Positive values towards the west and negative towards the east. Mean tidal flow is shown as dashed lines and the modal direction shown as circle markers. Boxes show the interquartile range (IQR, 25th and 75th percentiles) of  $\bar{V}$ . Whiskers represent the distance of 1.5 IQR from the 25th and 75th percentiles.

## 4. Results

### 4.1. Short term (seconds to days)

Offshore significant wave height ( $H_{s0}$ ) during the summer deployments was 1.5 m which is common for the study area; however  $H_{s0}$  values of approximately 3 m occurred during the winter deployments which is considered a low intensity, high frequency storm for the study area (NSWG, 1990). The nearshore wave heights ( $H_s$ ) were typically small throughout all surveys ( $\bar{H}_s \approx 0.25$  m) with larger  $H_s$  and longer wave periods ( $T$ ) during winter than during summer (Table 1). The largest  $H_s$  were observed in the exposed western end of the beach (SB3)

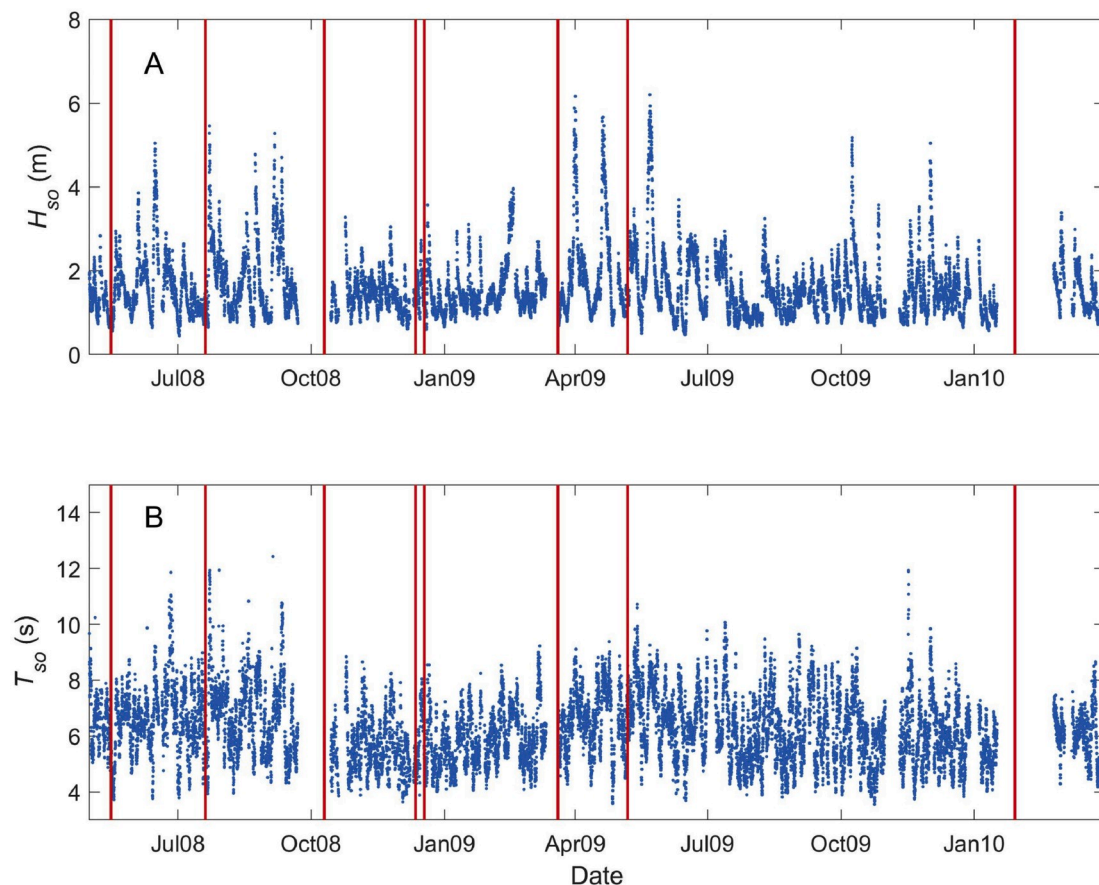


**Fig. 4.** Hourly wave data from Crowdy Head showing: A) significant wave height ( $H_{so}$ ); and, B) significant wave period ( $T_{so}$ ). Red vertical lines indicate the dates when the beach surveys were conducted. (For interpretation of the references to colour in this figure legend, the reader is referred to the Web version of this article.)

and were associated with the strongest longshore currents, double those observed at the protected (SB1) eastern end of the beach.

Current velocities at both locations varied depending on the stage of the tidal cycle with ebb tides generally causing westward currents and flood tides flowing eastward. This was most evident in the eastern location of the beach (SB1) where the mean net-current direction was near-zero. However, the modal and residual current direction was still predominantly to the west (Table 1, Fig. 3). The western environment (SB3) was less affected by tidal cycles and had westward trending currents throughout most of the measurement periods (Table 1, Fig. 3). Overall, longshore residual currents ( $R_f$ ) were generally from east to west at both stations during summer and winter conditions (Table 1), with stronger westward currents occurring in summer than in winter.

Direction of sediment entrainment ( $E_f$ ) mostly followed the trends of residual current direction being mostly westward directed (Table 1). However, disparity between  $R_f$  and  $E_f$  values occurred in the east with residual current direction opposing the direction of sediment entrainment during some deployments. This was due to instances where the dominant longshore current flow did not correspond with conditions where substantial sediment entrainment occurred since sediment entrainment was driven by nearshore wave orbital velocities and not average longshore current flow.

## 4.2. Medium term (seasons to years)

### 4.2.1. Offshore waves

Several storm events occurred during the study period (May 2008 to March 2010). Two severe storms occurred, one in April and one in May 2009 with their peak  $H_{so}$  greater than 6 m (Fig. 4). Another severe storm with  $H_{so}$  values above 5 m also occurred during April 2009. Moderate

storms ( $3.5 < H_{so} < 5$  m) occurred frequently throughout May to October 2008 and some in October and November 2009. High-frequency low-energy storms ( $3 < H_{so} < 3.5$  m) occurred during the rest of the study period (Fig. 4).

### 4.2.2. Beach volume change

Significant erosion occurred at Shoal Bay between May 2008 and January 2010 with approximately 19000 m<sup>3</sup> of sediment lost from the beach at a rate of 11000 m<sup>3</sup>yr<sup>-1</sup> and a shoreline retreat of approximately 1.1 myr<sup>-1</sup> (Fig. 5). The erosion observed was due a lowering or flattening of the beach face rather than erosion into the dune systems or dune retreat. There are four periods of significant volumetric change over the study period (Fig. 5): (a) July and October 2008 was the only period of accretion (5300 m<sup>3</sup>); (b) this then eroded between October and December 2008 (5700 m<sup>3</sup>); (c) The most significant loss of sediment then occurred between March and May 2009 (11000 m<sup>3</sup>) which was most of the volume change observed during the survey period (Fig. 5); and, (d) beach erosion of 5000 m<sup>3</sup> then occurred between May 2009 and January 2010. The surveys also revealed a substantial difference in beach size with the western area of the beach containing significantly more sediment than the other regions (Fig. 6). The digital elevation model (DEM) of the beach shows higher elevations in the west and also the prevalence of cusped features in this region (Fig. 6). The differences in beach size may also be partially explained by the lack of foredunes or berms in the central region of Shoal Bay. There is an erosion scarp but no dune system due to the proximity of infrastructure which has produced a flatter beach profile.

Shoreline erosion was most pronounced in the eastern and central sections of the beach (Sections 3-6) while the western sections underwent accretion (Sections 1 and 2) (Fig. 5). This suggests a general trend

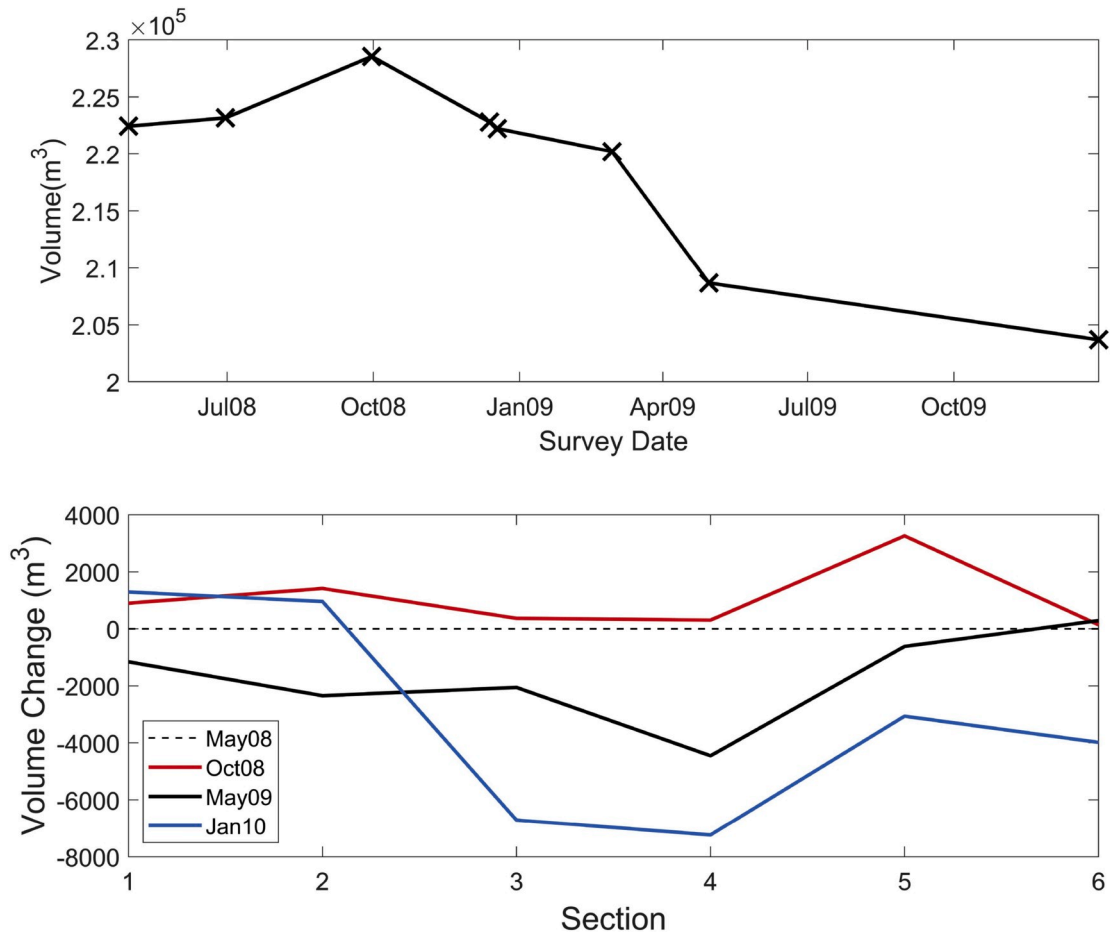


Fig. 5. A) Average beach volume for each survey and; B) volume change for four survey points (out of 8) between May 2008 and January 2010 for each section.

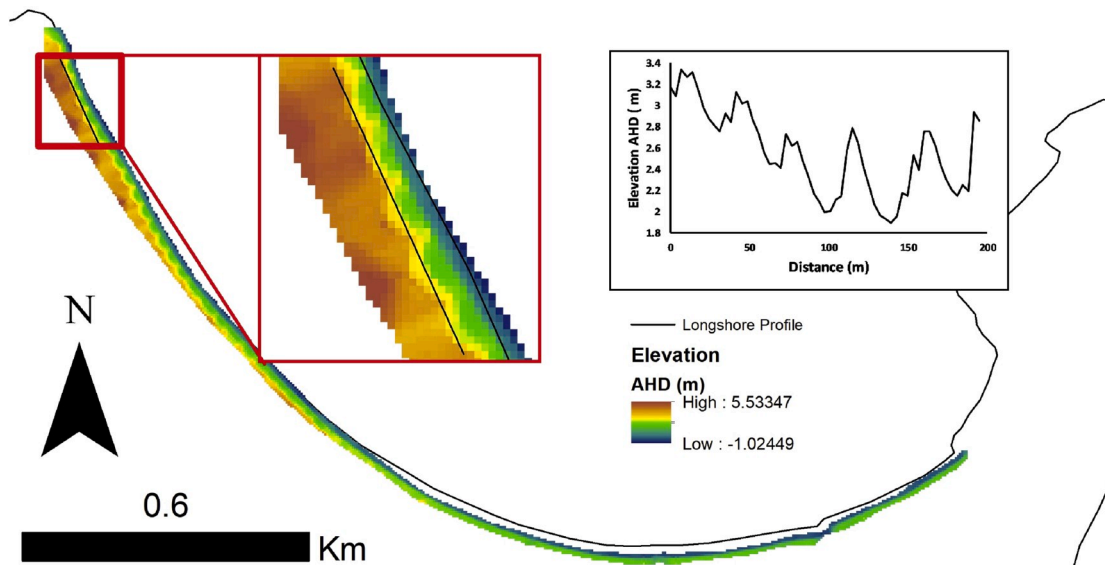


Fig. 6. Digital elevation model (DEM) of Shoal Bay beach during May 2009 with beach cusps apparent in the western area of the beach. A longshore profile shows the beach cusps that occur on the western area of the beach.

of westerly sediment movement in Shoal Bay that was supported by sediment grain-size and carbonate analysis conducted from samples collected on the beach face (Supplementary Material). The western sections were the only areas that accreted during the study period with about 1000 m³ of sediment accumulating between May 2008 and

January 2010; they showed typical summer and winter beach change, for the SE Australian coast, with erosion during winter and accretion during summer (Short, 2007). The central to eastern sections of the beach (3–5) responded in the opposite manner with erosion during summer and accretion during winter. This opposite response caused



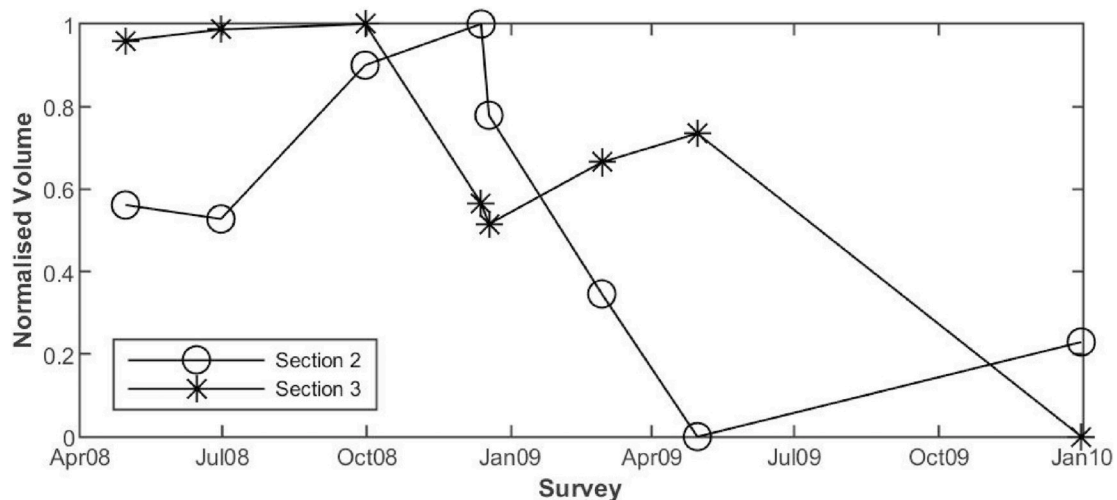


Fig. 7. Normalised volumes of beach sections 2 and 3 showing typical seasonal beach rotation in Shoal Bay.

Table 2

Erosion and accretion volumes error between the two bathymetric surveys and the average bed level change between October 2007 and February 2010. The volumes only include areas where bed level changes of greater than 0.2 m.

Region	Volume (m <sup>3</sup> )		Average Bed Level Change (m)	
	Net	m <sup>3</sup> yr <sup>-1</sup>	Net	myr <sup>-1</sup>
Ebb Shoal	-134000	-59821	-0.15	-0.07
Ebb Channel	-126000	-56250	-0.15	-0.07

beach rotation between the eastern and western sections of the beach (Fig. 7). However, erosion occurred independent of the seasonal behaviour due to the cluster of storms from the south-easterly direction between March and May 2009 that caused erosion along the entire beach.

The bathymetry showed erosion in both the ebb shoal and the ebb channel of the FTD, with similar rates of change in both areas (Table 2 and Fig. 1c). Erosion was not observed in all locations with areas of accretion also occurring related to the movement of bedforms (Fig. 1c).

#### 4.3. Long term (Years to decades)

##### 4.3.1. Offshore waves

The historic storm data from Sydney (Fig. 8) show clustering of storms between 1985 and 1991 followed by a period of lower storm activity that extended to the mid-1990s. Storm events increased again in 1995, 1999 and 2002 however when compared to the late 1980s the period from 1991 to 2006 was relatively calm. Most of the storms were from the southeast (between 90 and 180°) which will transmit wave energy into the entrance of Port Stephens estuary.

##### 4.3.2. Aerial photograph analysis

Analysis of shoreline change from four decades of aerial photography showed an erosive trend along the entire length of Shoal Bay. Each section of the beach retreated from the initial shoreline of 1963; however, the extent of shoreline retreat varies within the section (Fig. 9). The largest retreat occurred in both ends of the beach (sections 1-2 and 5-6), with smaller shoreline retreat observed in the central sections (sections 3-4).

Average shoreline retreat for the entire beach was 0.5 myr<sup>-1</sup> causing approximately 22 m of shoreline retreat (Fig. 9). Most of the retreat occurred between 1963 and 1977, the rest taking place during 1994-96 and 2001-06 after a period of stability and with small amounts of accretion between 1977-94 (Fig. 9). The largest rates of retreat occurred

between 1994 and 1996 with rate of shoreline change approximately -3.8 myr<sup>-1</sup>. During this period the shoreline retreated on average 9.3 m in 2.5 years (Fig. 9).

## 5. Discussion

Current direction and sediment entrainment in the nearshore zone was mainly driven by swell waves and tidal flows working simultaneously. Current direction was influenced by tidal stage and estuarine morphology, where flooding and ebbing tides flowed westward and eastward respectively. The nearshore flow direction in Shoal Bay is opposed to the direction of tidal currents at the estuary mouth due to a bathymetrically controlled eddy that develops because of the embayed shape of Shoal Bay (Jiang, 2012). However, the tidal influence on nearshore currents was weaker in the western area of the beach where the waves were the strongest suggesting that wave forcing was the major control influencing nearshore current direction (Table 1, Fig. 3). A characteristic of estuarine beaches is that, given their location in relation to the estuary entrance, swell waves can only arrive from the entrance. In this case, swell waves only arrive from the east creating westward wave-driven alongshore currents (Fig. 1). As a result, residual currents in the western region of Shoal Bay were dominated by wave driven westward currents instead of tidal flows (Table 1 Fig. 3). Most of the sediment entrainment also occurred in the more exposed regions due to the influence of swell waves that, in the wave-dominated microtidal area, have higher entrainment capability than the tidal currents (Table 1). Since the swell and tide conditions during the hydrodynamic deployments are common for Shoal Bay, it is likely that westward sediment transport dominates the nearshore zone most of the time. This is consistent with previous long-term studies in this type of estuary (Roy et al., 1980) and supported by sediment grainsize results for Shoal Bay (Supplementary Material).

The beach geomorphology shows the difference in wave energy exposure from east to west. Significantly larger beach morphology and well-formed beach cusps, indicative of higher energy conditions, are found in the western area of Shoal Bay (Fig. 6). In comparison, the central and eastern locations of Shoal Bay are indicative of low-energy beach environments with small beach widths, low elevation, and no pronounced rhythmic features on the beach face. The sediment dynamics and beach geomorphic change within Shoal Bay can also be differentiated into western/exposed and eastern/sheltered regions. This is shown in the seasonal differentials in erosion and accretion in the eastern and western regions of Shoal Bay resulting in beach rotation. During fair weather periods without storms most of the sediment moved westwards resulting in temporary erosion in the east and accretion in the



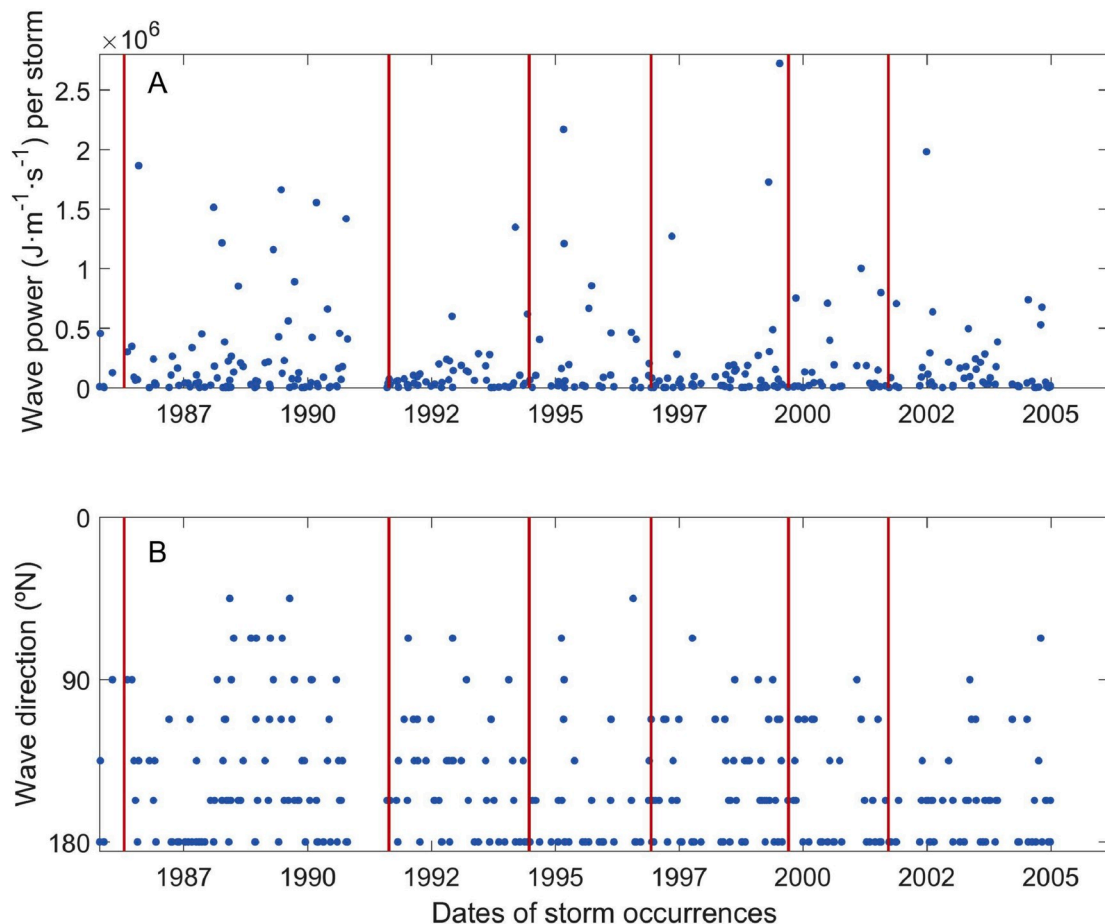


Fig. 8. Storm waves between 1985 and 2005 from the Sydney wave rider buoy showing A) Total wave power and B) Wave direction. Storm waves do not occur beyond 180° due to shoreline orientation. Red vertical lines correspond to dates of aerial photos used in this study. (For interpretation of the references to colour in this figure legend, the reader is referred to the Web version of this article.)

west (Figs. 4 and 7). However, greater swell wave energy during winter storm conditions correlated with erosion in the west and some accretion in the eastern regions of the beach (Figs. 4 and 7). Since the dominant direction of longshore sediment transport is towards the west we suggest the differentials between erosion and accretion in winter are driven primarily by cross-shore wave processes. This is similar to previous observations where cross-shore processes under storm swell drives seasonal differences between erosion and accretion cycles within an embayment (Harley et al., 2011, 2015). The seasonal processes driven by changes in wave climate in Shoal Bay led to beach rotation between the western and central/eastern locations (Fig. 7). Beach rotation is often considered to be the result of changes in swell wave direction (Short and Masselink, 1999); however this process is unlikely to occur in estuarine beaches since swell propagates through the mouth of the estuary and thus arrives from the same direction regardless of seasonal shifts in wave direction on the open coast. It is more likely that rotation in Shoal Bay is a function of both alongshore and cross-shore processes similar to those observed in open coast beaches (Harley et al., 2011, 2015). This is one of the first such observations for both estuarine and low-energy beaches since Nordstrom (1980) and it is indicative of the surprisingly dynamic beaches in the outer estuarine environment of Port Stephens (Vila-Concejo et al., 2011a). It further suggests that some of the insights on beach rotation from open coast environments (e.g. Harley et al., 2015), where waves are predominantly from one direction, could be applied in an estuarine beach setting where swell waves are still a dominant process.

During the winter storm period in southeast Australia the western area of Shoal Bay undergoes cross-shore driven erosion and recovers

during summer fair weather conditions via alongshore sediment input from the east. However, in the eastern areas erosion occurs during fair weather conditions with sediment transported to the western regions of Shoal Bay (October to February 2008 to 2009). Some recovery was observed during the winter storm period (March to May 2009) which may be due to the cross-shore transport of sediment from the FTD to the beach and potentially beach nourishment which was observed during the survey period although the volumes of sand placed are unknown. However, to more comprehensively investigate cross-shore driven transport topographic and bathymetric surveys that include information of sediment volume change in the nearshore zone are necessary as well as longer-term analysis of nearshore wave conditions. This would provide great insight into the specific drivers of cross-shore sediment dynamics on estuarine beaches which is a research topic with only a handful of studies.

Underlying the seasonal beach rotation was shoreline retreat observed at both short-term and long-term scales (Figs. 5 and 9). The severe storms between March and May 2009 resulted in erosion in almost all sections of the beach with a net loss of 10,000 m<sup>3</sup> of sediment (Figs. 4 and 5) with no recovery observed between May 2009 and January 2010 (Fig. 5). During the same period erosion was observed on the northern shoreline of Port Stephens with no recovery recorded (Vila-Concejo et al., 2010, 2011b). This erosion has likely continued in Port Stephens after the survey period in this study with qualitative observations of erosion of northern shoreline of Port Stephens into infrastructure in April 2015 and the establishment of new management plans in 2016 and sediment nourishment regimes in 2019 (Midcoast Council, 2019; SMEC, 2016). Previous studies in low-energy environments

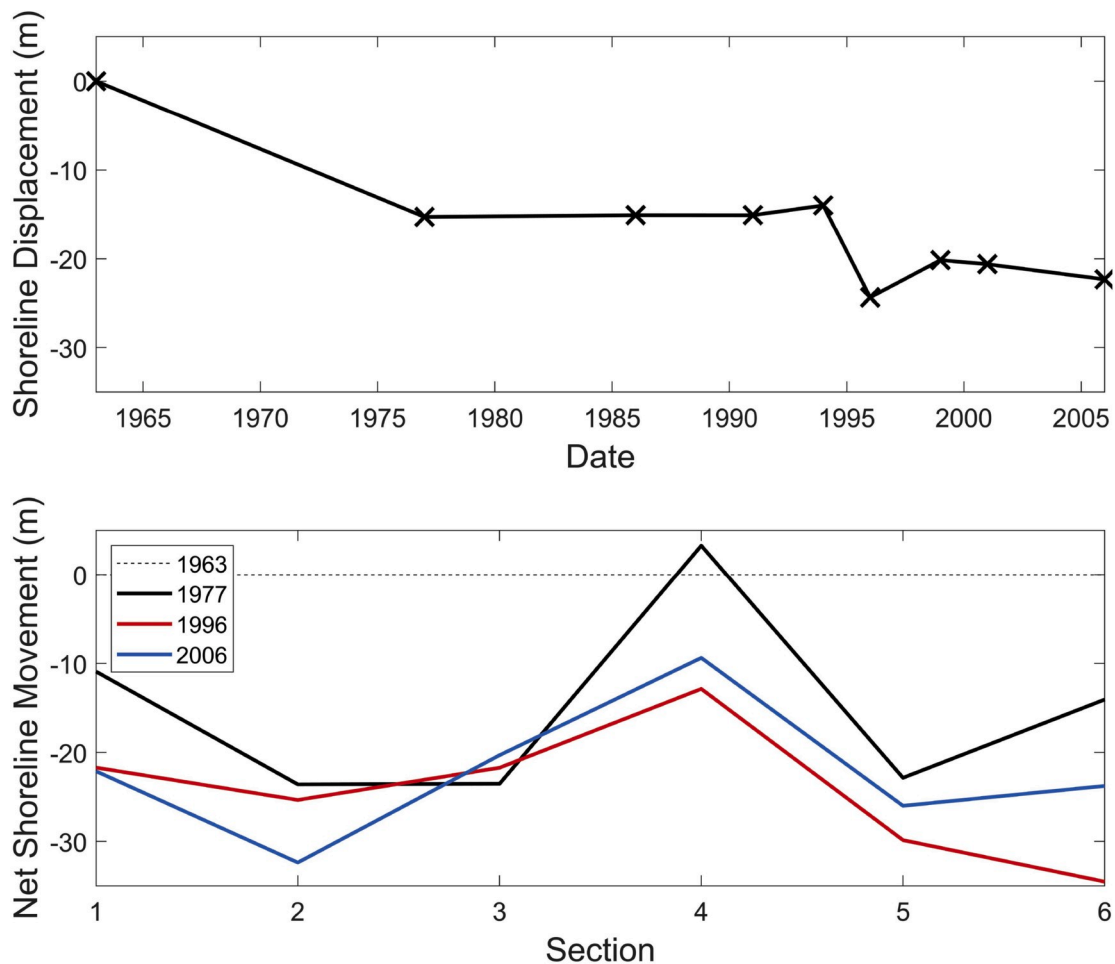


Fig. 9. A) Average long-term shoreline displacement from 1963 to 2006 and; B) net shoreline movement for four aerial photos (out of nine) over 43 years in each beach section.

suggest that complete recovery of the sediment lost due to storm events may not occur (e.g. Costas et al., 2005; Hegge et al., 1996; Sanderson et al., 2000; Travers, 2007) and is only possible with an extended period of fair weather conditions, if at all (Costas et al., 2005; Nordstrom, 1980; Owens, 1977). Shoreline recession was most pronounced in centre of the beach (Sections 3 and 4); with profiles in these areas undergoing parallel retreat that has been associated with beach change dominated by longshore transport (Nordstrom and Jackson, 1992). The location of the sediment lost from the beach during severe events is undetermined, but it is expected to have moved into deeper environments in the estuary or to have bypassed around the western headland of Shoal Bay. Bathymetric data indicate erosion in the features closest to Shoal Bay which suggests that headland bypassing under storm conditions is likely to have occurred. Austin et al. (2018) examined bathymetric change on a many features in Port Stephens over a similar period to this study and noted deflation/erosion in most surveyed locations in the estuary. However, given the gaps in the bathymetry data there may have been accumulation elsewhere in the estuary (Figs. 1c and 8, Table 2).

The erosion observed in the short- to medium-term analysis may offer insights into the processes driving long-term shoreline change in Shoal Bay. Long-term sediment imbalance is shown in the aerial photograph record in the form of shoreline retreat which has occurred for the last 43 years with few periods of accretion (Fig. 9). This retreat is most likely due to a long-term reduction in marine sediment input and movement of the FTD in Port Stephens resulting in the beach attempting to re-equilibrate by retreating (Austin et al., 2018). However, decadal beach change on Shoal Bay has been influenced by management and any

result should be viewed with this in mind. For example, the similar shoreline retreat distances (10–15 m) between 1963 and 1977 (14 years) and between 1977 and 2006 (39 years) is perhaps indicative of management interventions to maintain shoreline position since 1977. Yet, without detailed information for sediment volume change below mean sea level, quantifying the effect of beach nourishment interventions on shoreline position will remain challenging. Determining the exact process driving beach erosion, such as a reduced sediment input or a change in nearshore hydrodynamics, is also difficult without further in situ hydrodynamic measurements or long-term beach monitoring. However, future work could provide greater detail of the processes driving change by hind-cast modelling wave conditions in the estuary in combination with more recently developed shoreline change estimates using satellite records since 1979.

Nevertheless, the short to medium-term processes causing retreat are likely to be similar to those observed in this study, where high-energy storm events and westward directed sediment transport lead to a progressive reduction in sediment within Shoal Bay over time. Indeed storms are identified as both drivers of short-term erosion and agents of long-term shoreline retreat (Ferreira, 2005; Morton et al., 1995) particularly in low-energy (Backstrom et al., 2008; Tătui et al., 2014) and/or estuarine environments where sediment loss during severe storms is unlikely to be fully recovered (Costas et al., 2005; Hegge et al., 1996; Sanderson et al., 2000; Travers, 2007). Unless a substantive input of sediment from marine sources occurs in Shoal Bay the erosion observed in this study is likely to be continuous requiring constant nourishment to maintain shoreline position.

## 6. Conclusion

This paper presents a multi-scale assessment of the dynamics of an estuarine beach on a wave dominated coast. It provides insights into the factors that control sediment transport and long-term erosion of estuarine beaches influenced by flood-tide delta morphodynamics. The dynamics of Shoal Bay, from the data presented, can be interpreted by the following points:

- Fair weather summer conditions are dominated by alongshore westward sediment transport with erosion in the east and accumulation in the west.
- Winter storm conditions result in erosion in the west and some accretion in the east, most likely via cross-shore wave driven processes and supply of sediment from the flood-tide delta. Headland bypassing around the western headland is also likely to occur during winter.
- Differentials between erosion and accretion on the beach results in rotation over seasonal scales.
- Severe storms lead to wave-driven erosion across the entire beach. This is the likely event-based driver of chronic shoreline retreat observed over the last 40–50 years.
- A negative sediment flux has been persistent for decades and is most likely linked to the movement and erosion of the adjacent flood-tide delta.
- Maintenance of the Shoal Bay shoreline position will likely require continuous monitoring and nourishment.

The observations of beach rotation suggests that the dynamics of estuarine beaches can be similar to open coast environments. The long-term erosion of Shoal Bay is indicative of the complex sediment transport pathways and magnitudes in estuarine settings and highlights the need for further research into the interaction between FTDs and adjacent beaches. Future work in Port Stephens and similar settings should focus on building broader detailed sediment budgets and transport pathways in estuaries with a focus on the interactions between FTD and shoreline position perhaps via recent advances in remote sensing products. The different processes that drive change in estuaries; tide, wind, and swell waves, should be taken into account in future studies of estuarine beaches.

## Declaration of competing interest

The authors declare that they have no known competing financial interests or personal relationships that could have appeared to influence the work reported in this paper.

## CRediT authorship contribution statement

**Daniel L. Harris:** Conceptualization, Data curation, Writing - original draft, Methodology, Formal analysis, Investigation, Visualization. **Ana Vila-Concejo:** Conceptualization, Data curation, Writing - review & editing, Methodology, Investigation, Supervision, Project administration, Funding acquisition, Formal analysis. **Timothy Austin:** Conceptualization, Data curation, Writing - review & editing, Methodology, Investigation, Formal analysis. **Javier Benavente:** Conceptualization, Data curation, Writing - review & editing, Methodology, Investigation, Supervision, Formal analysis.

## Acknowledgements

We thank the three anonymous Reviewers for improved this manuscript. We also thank the field work team who helped collect data during the field campaigns in Port Stephens. DLH was funded by a UQ ECR (UQECR1946373) and New Staff Research Grant. This research was funded by the Australian Research Council (ARC) in collaboration with the Office of Environment and Heritage (OEH), a division of the NSW

Department of Premier and Cabinet (formerly the Department of Environment, Climate Change and Water (DECCW)), Great Lakes Council, Port Stephens Council and Jimmy's Beach Restoration Society Inc. through Linkage Grant LP0668979.

## Appendix A. Supplementary data

Supplementary data to this article can be found online at <https://doi.org/10.1016/j.ecss.2020.106759>.

## References

- Austin, T., Vila-Concejo, A., Short, A., Ranasinghe, R., 2018. A multi-scale conceptual model of flood-tide delta morphodynamics in micro-tidal estuaries. *Geosciences* 8, 324.
- Austin, T.P., Short, A.D., Hughes, M.G., Vila-Concejo, A., Ranasinghe, R., 2009. Tidal hydrodynamics of a micro-tidal, wave dominated flood-tide delta: Port Stephens, Australia. *J. Coast Res.* SI 56, 693–697. *Proceedings of the 10th International Coastal Symposium.*
- Backstrom, J., Jackson, D., Cooper, J., Malvarez, G., 2008. Storm-driven shoreface morphodynamics on a low-wave energy delta: the role of nearshore topography and shoreline orientation. *J. Coast Res.* 1379–1387.
- Benavente, J., Harris, D.L., Austin, T.P., Vila-Concejo, A., 2011. Medium term behavior and evolution of a beach cusps system in a low energy beach, Port Stephens, NSW, Australia. *J. Coast Res.* 170–174.
- Bernabeu, A.M., Lersundi-Kanpistegi, A.V., Vilas, F., 2012. Gradation from oceanic to estuarine beaches in a ria environment: a case study in the Ria de Vigo. *Estuarine, Coast. Shelf Sci.* 102–103, 60–69.
- Black, K., Healy, T., Hunter, M., 1989. Sediment dynamics in the lower section of a mixed sand and shell-lagged tidal estuary, New Zealand. *J. Coast Res.* 503–521.
- Boothroyd, J.C., 1985. Tidal inlets and tidal deltas. In: Davis Jr., R.A. (Ed.), *Coastal Sedimentary Environments*. Springer-Verlag New York Inc., New York, p. 420.
- Brander, R.W., Kench, P.S., Hart, D., 2004. Spatial and temporal variations in wave characteristics across a reef platform, Warraber Island, Torres Strait, Australia. *Mar. Geol.* 207, 169–184.
- Costas, S., Alejo, I., Vila-Concejo, A., Nombela, M.A., 2005. Persistence of storm-induced morphology on a modal low-energy beach : a case Study from NW-Iberian Peninsula. *Mar. Geol.* 224, 43–56.
- Cowell, P.J., Roy, P.S., Jones, R.A., 1995. Simulation of large-scale coastal change using a morphological behaviour model. *Mar. Geol.* 126, 45–61.
- Dalrymple, R.W., Zaitlin, B.A., Boyd, R., 1992. Estuarine facies models; conceptual basis and stratigraphic implications. *J. Sediment. Res.* 62, 1130–1146.
- DPWS, 1999. Port Stephens/Myall Lakes Estuary Processes Study. Manly Hydraulics Institute, Department of Public Works and Services. Report No. 913.
- DPWS, 2000. Jimmys Beach Coastline Management Review, Conceptual Sediment Budget and Beach Nourishment Practises.
- Ferreira, O., 2005. Storm groups versus extreme single storms: predicted erosion and management consequences. *J. Coast. Res.* SI 42, 221–227.
- Harley, M.D., Turner, I.L., Short, A.D., 2015. New insights into embayed beach rotation: the importance of wave exposure and cross-shore processes. *J. Geophys. Res.: Earth Surface* 120, 1470–1484.
- Harley, M.D., Turner, I.L., Short, A.D., Ranasinghe, R., 2010. Interannual variability and controls of the Sydney wave climate. *Int. J. Climatol.* 30, 1322–1335.
- Harley, M.D., Turner, I.L., Short, A.D., Ranasinghe, R., 2011. A reevaluation of coastal embayment rotation: the dominance of cross-shore versus alongshore sediment transport processes, Collaroy-Narrabeen Beach, southeast Australia. *J. Geophys. Res.* 116, F04033.
- Harris, D.L., Power, H.E., Kinsela, M.A., Webster, J.M., Vila-Concejo, A., 2018. Variability of depth-limited waves in coral reef surf zones. *Estuarine, Coast. Shelf Sci.* 211, 36–44.
- Hayes, M.O., 1975. Morphology of sand accumulation in estuaries. In: Cronin, L.E. (Ed.), *Estuarine Research*. Academic Press, New York, pp. 3–22.
- Hayes, M.O., 1980. General morphology and sediment patterns in tidal inlets. *Sediment. Geol.* 26, 139–156.
- Hegge, B., Eliot, I., Hsu, J., 1996. Sheltered sandy beaches of southwestern Australia. *J. Coast Res.* 12, 748–760.
- Jackson, N.L., Nordstrom, K.F., Eliot, I., Masselink, G., 2002. 'Low Energy' sandy beaches in marine and estuarine environments: a review. *Geomorphology* 48, 147–162.
- Jiang, A.W., 2012. Numerical Modelling of Flood-Tide Delta Morphodynamics at Port Stephens, New South Wales (NSW). PhD Thesis. School of Geosciences. University of Sydney.
- Karunaratna, H., Reeve, D., Spivack, M., 2008. Long-term morphodynamic evolution of estuaries: an inverse problem. *Estuar. Coast Shelf Sci.* 77, 385–395.
- Kench, P.S., Brander, R.W., 2006. Response of reef island shorelines to seasonal climate oscillations: south Maalhosmadulu atoll. Maldives. *J. Geophys. Res.* 111.
- Kench, P.S., McLean, R.F., 2004. Hydrodynamics and sediment flux of a lagoon in an Indian Ocean atoll. *Earth Surf. Process. Landforms* 29, 933–953.
- Lord, D., Kulmar, M., 2001. The 1974 storms revisited: 25 Years experience in ocean wave measurement along the south east Australian coast. In: *Coastal Engineering Conference*. ASCE American Society of Civil Engineers, pp. 559–572.

- Makaske, B., Augustinus, P.G.E.F., 1998. Morphologic change of a micro-tidal, low wave energy beach face during a spring-neap tide cycle, Rone Delta, France. *J. Coast Res.* 14, 632–645.
- Midcoast Council, 2019. Jimmys Beach sand transfer system is operational. <https://www.midcoast.nsw.gov.au/News-Media/Jimmys-Beach-sand-transfer-system-is-operational>. (Accessed 30 March 2020).
- Morton, R.A., Gibeaut, J.C., Paine, J.G., 1995. Meso-scale transfer of sand during and after storms: implications for prediction of shoreline movement. *Mar. Geol.* 126, 161–179.
- Nordstrom, K.F., 1980. Cyclic and seasonal beach response: a comparison of ocean and bayside beaches. *Phys. Geogr.* 1, 177–196.
- Nordstrom, K.F., Jackson, N.L., 1992. Two dimensional change on sandy beaches in estuaries. *Zeitschrift zur Geomorphologie* 36, 465–478.
- Nordstrom, K.F., Jackson, N.L., Allen, J.R., Sherman, D.J., 2003. Longshore sediment transport rates on a microtidal estuarine beach. *J. Waterw. Port, Coast. Ocean Eng.* 129, 1–4.
- NSWG, 1990. Coastline Management Manual. NSW Government.
- Owens, E.H., 1977. Temporal variations in beach and nearshore dynamics. *J. Sediment. Petrol.* 47, 168–190.
- Perillo, G., Piccolo, M., 2011. Global variability in estuaries and coastal settings. *Treatise Estuarine Coast. Sci.* 7–36.
- PWD, 1979. Nelson Bay Erosion Study, p. 79003.
- PWD, 1985. Jimmys Beach Management Report. Great Lakes Shire Council in conjunction with Public Works Department New South Wales. Report No. 85012.
- PWD, 1987. Jimmys Beach Erosion Study, p. 85042.
- Roy, P.S., 1984. New South Wales estuaries: origin and evolution. In: Thom, B.G. (Ed.), *Coastal Geomorphology in Australia*. Academic Press Australia, North Ryde.
- Roy, P.S., 2001. Sand Deposits of the NSW Inner Continental Shelf. Report to Coastal Council of NSW, Geoscience Surveys.
- Roy, P.S., Thom, B.G., Wright, L.D., 1980. Holocene sequences on an embayed high-energy coast: an evolutionary model. *Sediment. Geol.* 26, 1–19.
- Roy, P.S., Williams, R.J., Jones, A.R., Yassini, I., Gibbs, P.J., Coates, B., West, R.J., Scanes, P.R., Hudson, J.P., Nichol, S., 2001. Structure and function of south-east Australian estuaries. *Estuarine. Coast. Shelf Sci.* 53, 351–384.
- Sanderson, P.G., Eliot, I., Hegge, B., Maxwell, S., 2000. Regional variation of coastal morphology in southwestern Australia: a synthesis. *Geomorphology* 34, 73–88.
- Shand, T., Goodwin, I., Mole, M., Carley, J., Browning, S., Coghlan, I., Harley, M., Pierson, W., Kulmar, M., 2010. NSW Coastal Storms and Extreme Waves. University of New South Wales, Sydney, Australia. Water Research Laboratory Technical Report.
- Short, A.D., 2006. Australian beach systems: nature and distribution. *J. Coast Res.* 22, 11–27.
- Short, A.D., 2007. *Beaches of the New South Wales Coast*, second ed. Sydney University Press, Sydney.
- Short, A.D., Masselink, G., 1999. Embayed and structurally controlled beaches morphodynamics. In: Short, A.D. (Ed.), *Handbook of Beach and Shoreface Morphodynamics*. John Wiley and Sons, Ltd, Chichester, pp. 230–249.
- Short, A.D., Trenaman, N.L., 1992. Wave climate of the Sydney region, an energetic and highly variable ocean wave regime. *Aust. J. Mar. Freshw. Res.* 43, 765–791.
- SMEC, 2016. Jimmys Beach Coastal Zone Management Plan.
- Soulsby, R.L., 1997. *Dynamics of Marine Sands: A Manual for Practical Applications*. Thomas Telford, London.
- Tătu, F., Vespremeanu-Stroe, A., Preoteasa, L., 2014. Alongshore variations in beach-dune system response to major storm events on the Danube Delta coast. *J. Coast Res.* 70, 693–700.
- Thieler, E.R., Himmelstoss, E.A., Zichichi, J.L., Ayhan, E., 2009. Digital Shoreline Analysis System (DSAS) Version 4.0 - an ArcGIS Extension for Calculating Shoreline Change: U.S. Geological Survey Open-File Report 2008-1278.
- Thom, B.G., Shepard, M., Ly, C.K., Roy, P.S., Bowman, G.M., Hesp, P.A., 1992. *Coastal Geomorphology and Quaternary Geology of the Port Stephens/Myall Lakes Area*. Department of Biogeography and Geomorphology, Australian National University, Canberra.
- Travers, A., 2007. Low-energy beach morphology with respect to physical setting: a case study from cockburn sound, southwestern Australia. *J. Coast Res.* 23, 429–444.
- Vila-Concejo, A., Austin, T.P., Harris, D.L., Hughes, M.G., Short, A.D., Ranasinghe, R., 2011a. Estuarine beach evolution in relation to a flood-tide delta. *J. Coast Res.* 190–194.
- Vila-Concejo, A., Austin, T.P., Harris, D.L., Hughes, M.G., Short, A.D., Ranasinghe, R., 2011b. Estuarine beach evolution in relation to a flood-tide delta. *J. Coast Res.* 190–194.
- Vila-Concejo, A., Gallop, S.L., Largier, J., 2019. Sandy beaches in estuaries and bays. In: Jackson, D., Short, A.D. (Eds.), *Sandy Beach Morphodynamics*. Accepted.
- Vila-Concejo, A., Hughes, M.G., Short, A.D., Ranasinghe, R., 2010. Estuarine shoreline processes in a low-energy system. *Ocean Dynam.* 60, 285–298.
- Vila-Concejo, A., Short, A.D., Hughes, M.G., Ranasinghe, R., 2007. Flood-tide delta morphodynamics and management implications, Port Stephens, Australia. *J. Coast Res.* 705–709. SI 50 (Proceedings of 9th International Coastal Symposium).
- Vila-Concejo, A., Short, A.D., Hughes, M.G., Ranasinghe, R., 2009. Formation and evolution of a sandwave on an estuarine beach. *J. Coast Res.* SI 56, 153–157.
- Webb, A., 2006a. An Analysis of Coastal Change and Erosion - Tebunginako Village, Abaiang, Kiribati. South Pacific Applied Geoscience Commission (SOPAC). Technical Report 53.
- Webb, A., 2006b. Coastal Change Analysis Using Multi-Temporal Image Comparisons - Funafuti Atoll. South Pacific Applied Geoscience Commission (SOPAC). Technical Report 54.
- Winter, G., Lowe, R., Symonds, G., Hansen, J., van Dongeren, A., 2017. Standing infragravity waves over an alongshore irregular rocky bathymetry. *J. Geophys. Res.: Oceans* 122, 4868–4885.
- Wright, L.D., Short, A.D., 1984. Morphodynamic variability of surf zones and beaches: a synthesis. *Mar. Geol.* 56, 93–118.